



OPEN ACCESS

EDITED BY

Wenguang Wang,
Northeast Petroleum University, China

REVIEWED BY

Xushan Lu,
Shandong University, China
Zhengyu Xu,
Chongqing University, China

*CORRESPONDENCE

Lei Zhou,
✉ 501161@yangtzeu.edu.cn

RECEIVED 01 March 2024

ACCEPTED 21 March 2024

PUBLISHED 09 April 2024

CITATION

Zhang W, Xie X, Zhou L, Wang X and Yan L (2024), 3-D forward modeling of shale gas fracturing dynamic monitoring using the borehole-to-ground transient electromagnetic method. *Front. Earth Sci.* 12:1394094. doi: 10.3389/feart.2024.1394094

COPYRIGHT

© 2024 Zhang, Xie, Zhou, Wang and Yan. This is an open-access article distributed under the terms of the [Creative Commons Attribution License \(CC BY\)](https://creativecommons.org/licenses/by/4.0/). The use, distribution or reproduction in other forums is permitted, provided the original author(s) and the copyright owner(s) are credited and that the original publication in this journal is cited, in accordance with accepted academic practice. No use, distribution or reproduction is permitted which does not comply with these terms.

3-D forward modeling of shale gas fracturing dynamic monitoring using the borehole-to-ground transient electromagnetic method

Weihao Zhang^{1,2}, Xingbing Xie^{1,2}, Lei Zhou^{1,2*}, Xinyu Wang³ and Liangjun Yan²

¹Key Laboratory of Exploration Technology for Oil and Gas Resources (Yangtze University), Ministry of Education, Wuhan, China, ²Cooperative Innovation Center of Unconventional Oil and Gas, Yangtze University, Wuhan, Hubei, China, ³School of Geophysics and Geomatics, China University of Geosciences, Wuhan, China

The borehole-ground transient electromagnetic method enhances the detection range and resolution by placing the transmitter electrode within the borehole, allowing for close-proximity excitation of subsurface targets and compensating for the shortcomings of traditional ground-based methods. Utilizing an unstructured vector finite element method combined with a second-order backward Euler variable time-stepping difference scheme and the MUMPS solver, we have achieved three-dimensional forward modeling simulation of the transient electromagnetic field for a borehole-ground electric source. Based on the validation of its accuracy, we analyzed the effectiveness of this method for dynamic monitoring of shale gas reservoir fracturing. Through forward modeling, we examined the characteristics of the radial electric field response during shale gas reservoir fracturing monitoring and evaluated the effectiveness of the borehole-ground TEM method in dynamic monitoring of shale gas reservoirs. The research results indicate that this method can meet the requirements for reservoir fracturing dynamic monitoring and has a promising application prospect.

KEYWORDS

borehole transient electromagnetic method, finite element, three-dimensional forward modeling, dynamic monitoring, shale gas fracturing

1 Introduction

In recent years, as unconventional oil and gas utilization enter a late stage of development into areas where the water cut is high, research on the identification of oil, gas, and water; the prediction of the residual oil and gas distribution; and the dynamic monitoring of oil reservoirs has become crucial (Hu et al., 2014; Zhao et al., 2019). Hydraulic fracturing is a key technology in the development of unconventional oil and gas reservoirs that directly affects the production of unconventional oil and gas. The forward simulation of hydraulic fracturing dynamic monitoring models can not only verify the effectiveness of hydraulic fracturing, but also provides important guidance for the hydraulic fracturing of unconventional oil and gas. Although techniques such as the time-lapse seismic method have matured, during hydraulic fracturing, the small difference in the acoustic impedance

caused by the displacement of reservoir fluids by fracturing fluids makes data interpretation difficult, and this method is also costly. Therefore, geophysical methods such as time-lapse gravity and time-lapse electromagnetic models are beginning to be developed (Peng et al., 2012). Notably, the displacement of fracturing fluids can cause significant changes in reservoir electrical properties, providing a theoretical basis for the application of electromagnetic exploration techniques in the dynamic monitoring of unconventional oil and gas reservoirs.

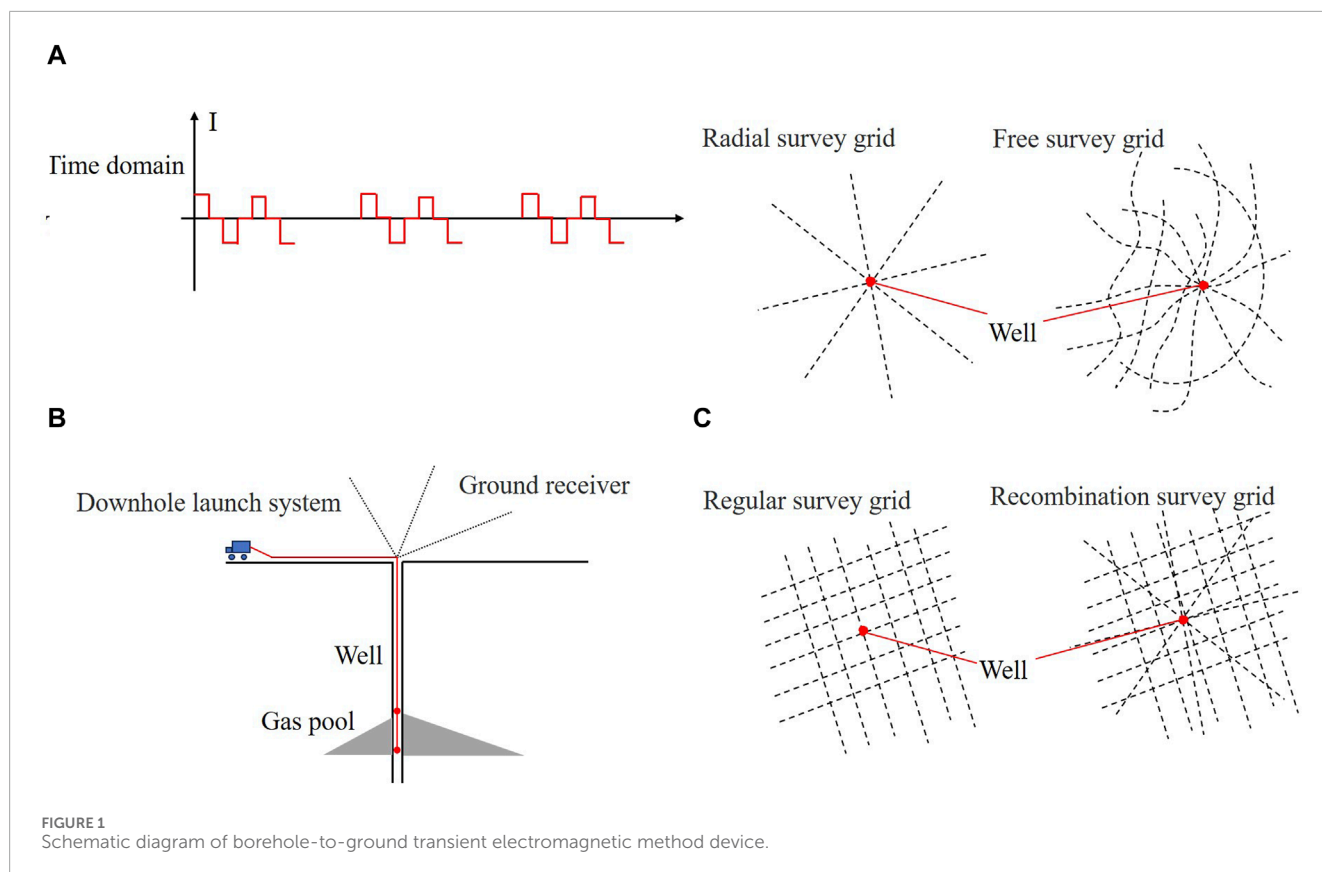
With the increasing demand for the exploration of deep-seated resources, several limitations in conventional ground-based electromagnetic surveying techniques for deep resource exploration have been identified. To address these issues, two approaches can be pursued. First, increasing the transmit power of the excitation field source to improve the signal-to-noise ratio of the received electromagnetic signals can enhance the practicality and effectiveness of electromagnetic methods. Second, facilities such as tunnels, mines, and boreholes can be used to place a transmitter under-ground and close to the target body for emission stimulation. This not only allows for the acquisition of stronger abnormal response signals, thereby increasing the detection depth, but also enhances the resolution of the abnormal body.

The transient electromagnetic method has been widely applied in environmental surveys, oil and gas exploration, mineral exploration, geothermal resource exploration, and deep crustal studies. Compared to controlled-source electromagnetic (CSEM) and magnetotelluric (MT) methods, this method has several advantages, such as a greater detection depth and a higher signal-to-noise ratio (Keller et al., 1984; Strack, 1984; Hördt et al., 1992; Mitsuhashi et al., 2002; Müller et al., 2002; Commer et al., 2006; Haroon et al., 2015; He and Xue, 2018). The rational interpretation of electromagnetic data relies on forward and inversion techniques, and forward simulation plays a crucial role by providing important guidance for oil and gas reservoir development. Therefore, this topic has been the focus of widespread attention by scholars.

Current research on time-domain electromagnetic methods primarily focuses on numerical simulation and feasibility analysis. In the field of borehole transient electromagnetic technology, the borehole electrical method was initially proposed by researchers in the former Soviet Union for the delineation of coal seam horizons. He Zhanxiang further developed the borehole time-frequency electromagnetic method based on previous research, deriving a three-dimensional numerical simulation algorithm for vertical dipole sources using the volume integral equation method, and achieved three-dimensional forward and inversion modeling of borehole electromagnetic methods (Wang et al., 2006; Wang et al., 2007). Ke Ganpan and Huang Qinghua used finite element methods to implement three-dimensional forward simulation of vertical line source electric fields (Ke and Huang, 2009). Cuevas established a borehole electromagnetic model that involved placing vertical electric dipole sources as excitation sources at the bottom of the metal casing. In addition, Cuevas analyzed the electromagnetic response characteristics at the radial distance measurement points on the ground and studied the effects of factors such as the length

and conductivity of the metal casing on the response (Cuevas, 2012). Ghada and Sami conducted time-domain numerical simulations of infinitely long wire sources in two-layered formations and analyzed the influences of different layer conductivities on the response results (Ghada and Al-Najim, 2015). Zhang Jiaqi integrated the expressions for each component of the dipole electromagnetic field along the direction of the wire to obtain analytical expressions for the vertical long wire source's electromagnetic field, and compared the responses of this field with the response of the ground horizontal electric dipole as part of a three-dimensional forward simulation of a borehole. This demonstrated the significant advantages of borehole electromagnetic methods in deep resource detection compared to conventional ground-based methods (Zhang, 2018). In terms of dynamic monitoring, Orange et al. analyzed the feasibility of using marine controlled-source electromagnetic methods to monitor the process of oil and gas reservoir development based on a classic two-dimensional oil and gas model (Orange et al., 2009). Furthermore, Wirianto et al. studied the feasibility of using land-based controlled-source electromagnetic methods to monitor changes in oil and gas reservoirs through numerical simulations of complex three-dimensional resistivity models (Wirianto et al., 2010). Meanwhile, Xie Xingbing et al. conducted experiments on residual oil monitoring using time-domain long-offset transient electromagnetic methods and preliminarily verified the effectiveness of this method in detecting residual oil boundaries (Xie et al., 2016). Li et al. proposed a multi-source, multi-directional ground-to-well vertical electromagnetic profiling method and used the integral equation method to simulate the electromagnetic response characteristics of oil and gas reservoir resistivity and oil saturation changes during water injection and production processes (Li et al., 2017). Liu et al. conducted numerical simulations and field experiments on the hydraulic fracturing process of shale gas fields and confirmed the good effect of controlled-source electromagnetic methods in monitoring shale gas production (Liu R. et al., 2020). Wang Xinyu et al. conducted a simulation and performed an analysis of the dynamic monitoring of oil reservoirs using electrical source transient electromagnetic methods and verified the significant response effects of this method in the dynamic monitoring of oil and gas reservoirs (Wang et al., 2022).

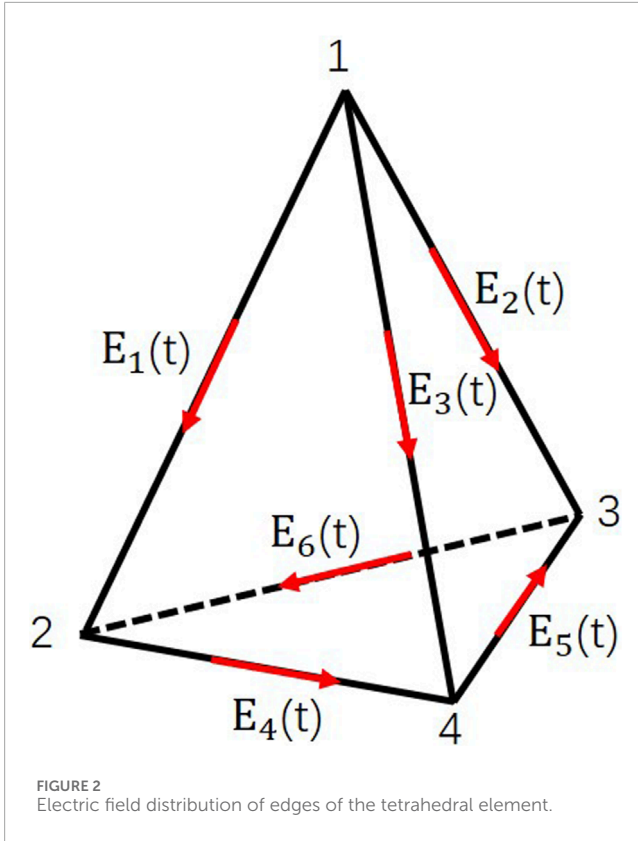
Early studies have demonstrated that, compared to conventional ground-based electromagnetic methods, borehole electromagnetic methods have significant advantages in deep exploration. Additionally, electrical source transient electromagnetic methods have been proven to be feasible for the dynamic monitoring of reservoirs. Therefore, based on the non-structured vector finite element method, in this paper, a borehole model is constructed, and the finite element results are compared with numerical filtering solutions to validate the algorithm's effectiveness. Subsequently, we establish a three-dimensional model and calculate the electric field components for dynamic monitoring of shale gas hydraulic fracturing within the model and analyze the relative anomaly changes to verify the effectiveness of borehole transient electromagnetic methods in the dynamic monitoring of shale gas hydraulic fracturing.



2 Method and technique of the dynamic monitoring of shale gas fracturing using the time domain electromagnetic method

In recent years, the borehole electromagnetic method has emerged as a widely applied electromagnetic method in the exploration of oil and gas reservoirs, residual oil detection in oil fields, and the dynamic monitoring of reservoirs. It mainly consists of two forms: 1) the well-surface electromagnetic method (WSEM), in which electromagnetic sources are emitted from within the well and received on the surface; and 2) the surface-well-electromagnetic method (SWEM), in which electromagnetic sources are emitted from the surface and received within the well. In the borehole electromagnetic method, the casing of the well can be used as the emitting electrode, or else dipole/magnetic sources can be placed near the geological target layer within the well for close-range stimulation. The excitation signal can be single-frequency or multi-frequency domain electromagnetic waves, or alternatively, it can be time-domain square waves. Array observations are conducted on the ground to measure the intensity of the electric field and the induced electromotive force components. The measured signal strength depends on the distribution of the formation resistivity and other physical parameters within the electromagnetic field's range of action determined by the observation method (Hu et al., 2022).

The transmitter of the borehole transient electromagnetic method is either an electrode (electrical source) or a magnetic dipole source (magnetic source) located in the well. The waveform of the transmitted current can be a zero-based square wave or a pseudo-Gaussian pulse, and the source can be moved within the well to conduct measurements. The receiving array can be deployed in various layouts depending on the surface conditions. At each excitation point, signals from multiple excitation cycles need to be observed and stacked to improve the signal-to-noise ratio, which requires more measurement time than the charging method. Both the electric field components and magnetic field components can be measured simultaneously to compensate for the insensitivities of electric and magnetic fields to different electrical differences. In addition to imaging the intensity and gradient of the electric field, processing of the observation data can also yield images of the apparent resistivity and polarization parameters of the target interval. The borehole transient electromagnetic method has been widely used in the study of various factors, such as the layering of oil and gas reservoirs, the delineation of reservoirs, and the exploration of underground water. It is characterized by its high efficiency, easy operation, and fast exploration speed. Compared to surface-well electromagnetic methods and airborne electromagnetic methods, borehole electromagnetic methods have a broader exploration range and are more sensitive to high-resistivity anomalies. The borehole transient electromagnetic detection method is an effective electromagnetic exploration method (Figure 1) (Hu et al., 2022).



3 Implementation of 3-D forward algorithm

3.1 Time domain finite element forward modeling theory of electromagnetic fields

In the quasi-static state, the time domain Maxwell equations of the active region can be expressed as follows:

$$\nabla \times \mathbf{E}(\mathbf{r}, t) = -\frac{\partial \mathbf{B}(\mathbf{r}, t)}{\partial t} \quad (1)$$

$$\nabla \times \mathbf{H}(\mathbf{r}, t) = \mathbf{J}(\mathbf{r}, t) + \mathbf{J}_s(\mathbf{r}, t) \quad (2)$$

$$\nabla \cdot (\mathbf{J}(\mathbf{r}, t) + \mathbf{J}_s(\mathbf{r}, t)) = 0 \quad (3)$$

Starting from the Maxwell equations in the time domain, the magnetic field is eliminated, and the electric field diffusion equation, which ignores the displacement current term, is established:

$$\nabla \times \left(\frac{1}{\mu} \nabla \times \mathbf{E}(\mathbf{r}, t) \right) + \sigma \frac{\partial \mathbf{E}(\mathbf{r}, t)}{\partial t} + \frac{\partial \mathbf{J}_s(\mathbf{r}, t)}{\partial t} = 0 \quad (4)$$

where μ is the permeability; \mathbf{r} is the position vector; $\mathbf{E}(\mathbf{r}, t)$ is the electric field intensity at position \mathbf{r} , at time t ; $\mathbf{H}(\mathbf{r}, t)$ is the magnetic field intensity at position \mathbf{r} , at time t ; $\mathbf{B}(\mathbf{r}, t)$ is the magnetic induction intensity at position \mathbf{r} , at time t ; $\mathbf{J}(\mathbf{r}, t)$ is the conduction current density at position \mathbf{r} , at time t ; $\mathbf{J}_s(\mathbf{r}, t)$ is the applied source current density at position \mathbf{r} , at time t ; and σ is the electrical conductivity.

An unstructured tetrahedral grid is used to discretely calculate the region, and the Nédélec vector interpolation basis function,

which automatically satisfies the continuity and non-dispersion of the tangential component of the electric field, is used to approximate the linear distribution of the electric field within the element. (Figure 2) The electric field inside any tetrahedral element can be expressed as follows:

$$\mathbf{E}(\mathbf{r}, t) = \sum_{j=1}^6 E_j(t) \mathbf{N}_j(\mathbf{r}) \quad (5)$$

where $E_j(t)$ is the tangential electric field value on the j edge of the tetrahedral element, which can be called the degree of freedom, and $\mathbf{N}_j(\mathbf{r})$ is the vector interpolation basis function.

Based on Galerkin's weighted margin method and Eq. 5, the following equation can be obtained:

$$\begin{aligned} & \iiint_{\Omega} \omega(\mathbf{r}) \cdot \nabla \times \left(\frac{1}{\mu} \nabla \times \mathbf{E}(\mathbf{r}, t) \right) dv + \iiint_{\Omega} \omega(\mathbf{r}) \cdot \sigma \frac{\partial \mathbf{E}(\mathbf{r}, t)}{\partial t} dv \\ & + \iiint_{\Omega} \omega(\mathbf{r}) \cdot \frac{\partial \mathbf{J}_s(\mathbf{r}, t)}{\partial t} dv = 0 \end{aligned} \quad (6)$$

Finally, an equation in the following form is obtained:

$$\mathbf{S}\mathbf{E}(t) + \mathbf{M} \frac{d\mathbf{E}(t)}{dt} = -\mathbf{J} \quad (7)$$

where \mathbf{S} and \mathbf{M} are the global stiffness matrix and mass matrix, and \mathbf{J} is the source term. The specific expression is as follows:

$$\mathbf{S} = \frac{1}{\mu} \iiint_{\Omega} (\nabla \times \mathbf{N}(\mathbf{r})) \cdot (\nabla \times \mathbf{N}(\mathbf{r})) dv \quad (8)$$

$$\mathbf{M} = \iiint_{\Omega} \mathbf{N}(\mathbf{r}) \cdot \sigma \cdot \mathbf{N}(\mathbf{r}) dv \quad (9)$$

$$\mathbf{J} = \iiint_{\Omega} \mathbf{N}(\mathbf{r}) \cdot \frac{\partial \mathbf{J}_s(\mathbf{r}, t)}{\partial t} dv \quad (10)$$

where v is the volume of the unit. For a grounded vertical long wire source, we approximate it to a superposition of multiple segments of electric dipoles (Ansari and Farquharson, 2014), each of which can be expressed as follows:

$$\mathbf{J}_s(\mathbf{r}, t) = I(t) \mathbf{u} \delta(\mathbf{r} - \mathbf{r}_s) dl \quad (11)$$

where $I(t)$ is the current intensity at time t , dl is the length of the electric dipole, \mathbf{u} is the current direction vector, \mathbf{r}_s is the position of the emission dipole source, and δ is an impulse function.

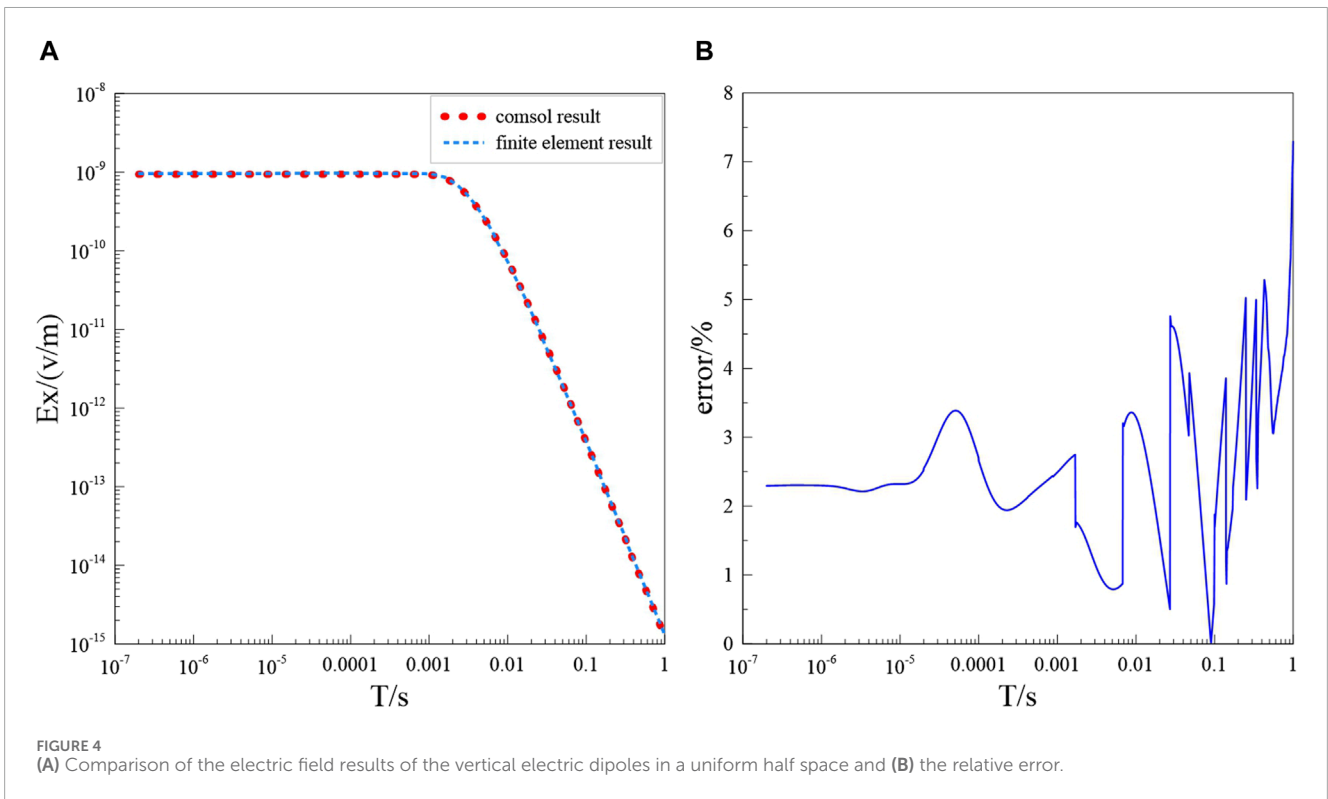
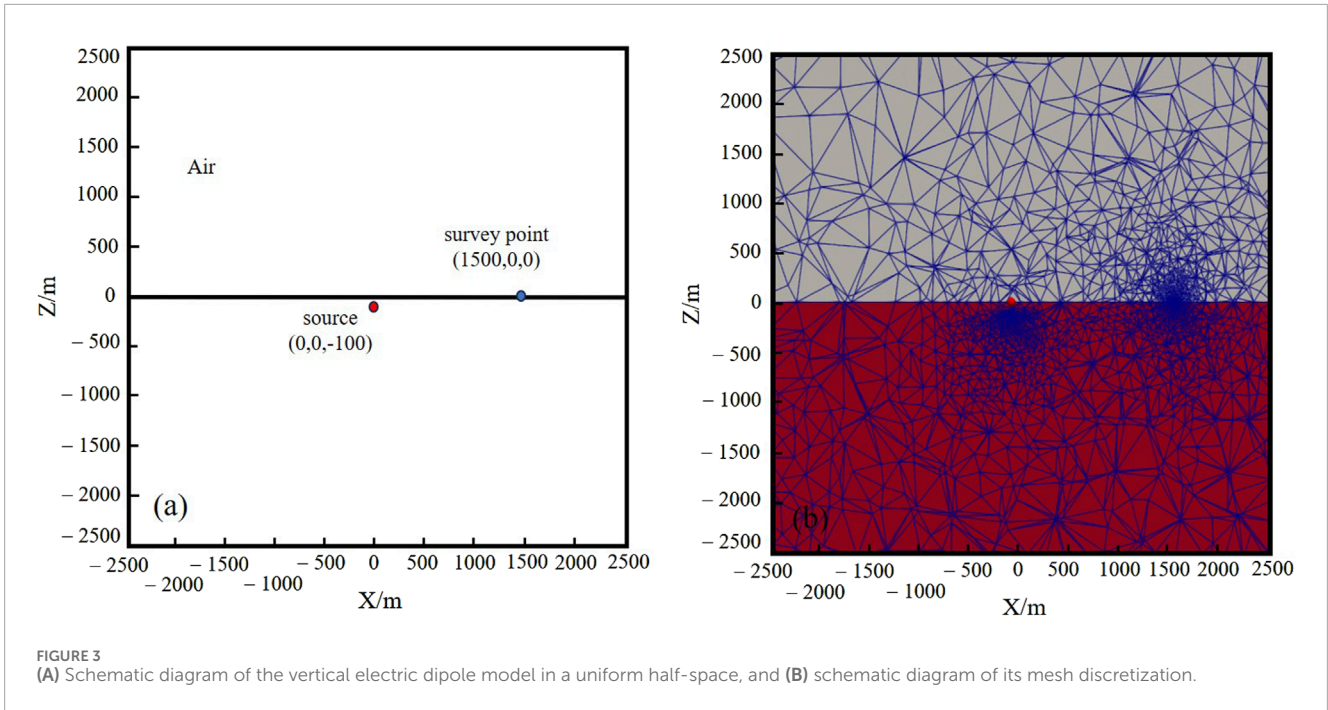
In order to improve the numerical accuracy, the time is discretized using the second-order backward Euler difference scheme, and simultaneous Eq. 7 (Um et al., 2010):

$$(3\mathbf{S} + 2\Delta t \mathbf{M}) \mathbf{E}_i(t) = \mathbf{S} [4\mathbf{E}^{i-1}(t) - \mathbf{E}^{i-2}(t)] - 2\Delta t \mathbf{J}^i \quad (12)$$

Finally, large linear equations are formed, which can be expressed as follows:

$$\mathbf{K}\mathbf{E} = \mathbf{b} \quad (13)$$

In order to solve Eq. 13, the initial electric field $\mathbf{E}(\mathbf{r}, 0)$ at time $t = 0$ should be given. For a series of current sources with an initial current of zero, such as a grounded long wire source, square wave, triangle wave, sine wave, or trapezoid wave, the initial electric field is $\mathbf{E}(\mathbf{r}, 0) = 0$. The initial electric field of the next step waveform is composed of two parts: the spatial electric field distribution caused



by the long wire source and the stable direct current electric field formed by the positive and negative electrodes.

$$\mathbf{E}(\mathbf{r}, 0) = \mathbf{E}_L(\mathbf{r}) - \mathbf{E}_{DC}(\mathbf{r}) \tag{14}$$

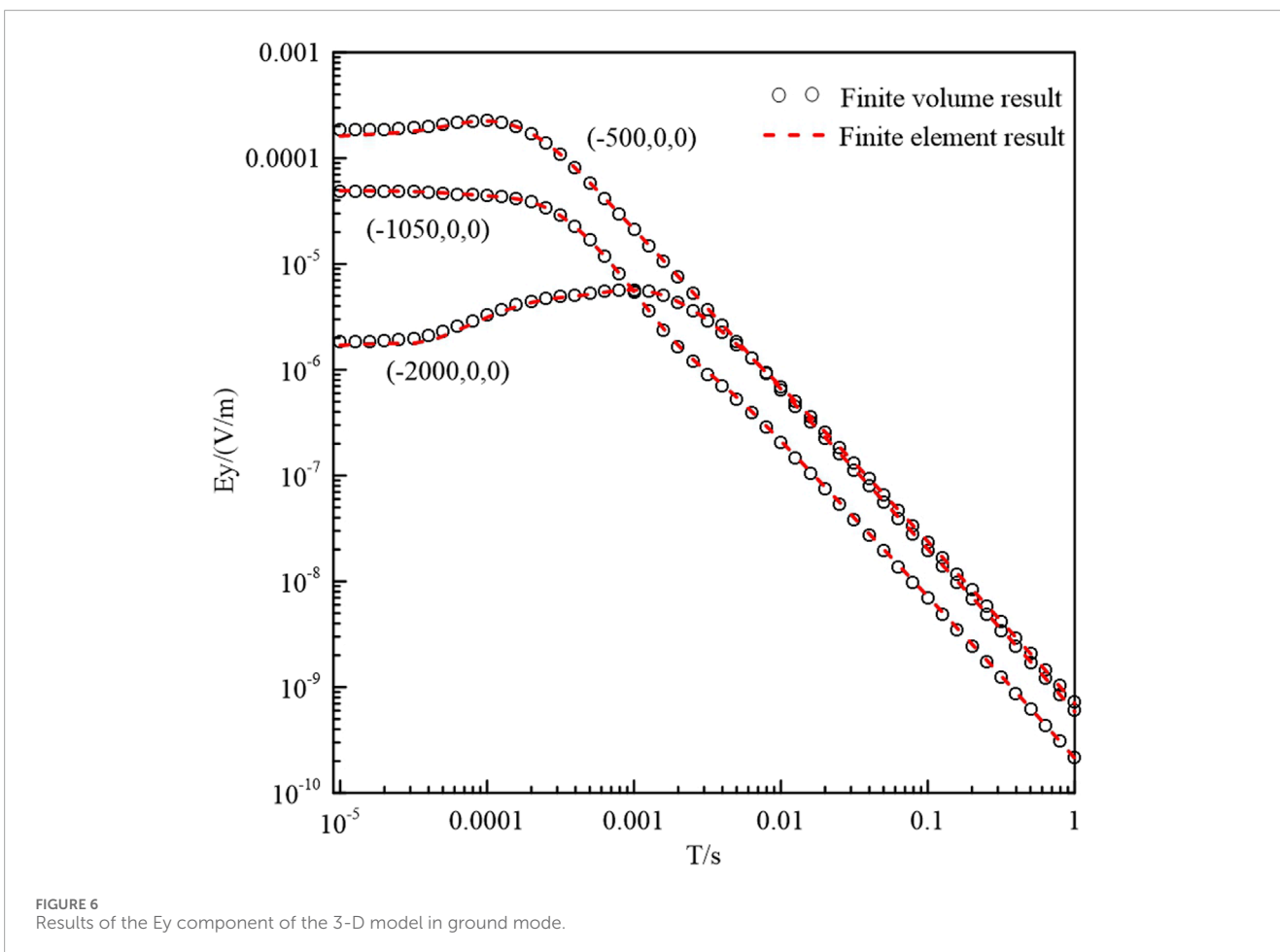
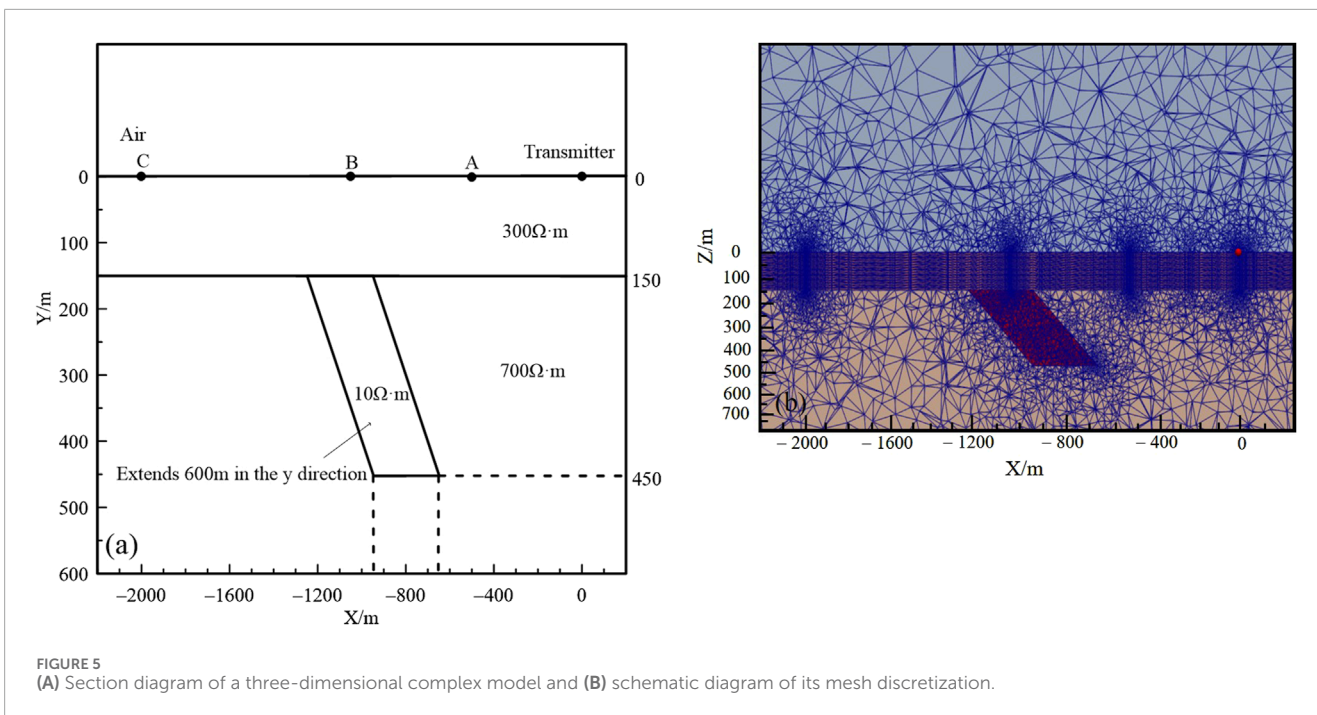
$\mathbf{E}_L(\mathbf{r})$ can be calculated from Ohm's law, and $\mathbf{E}_{DC}(\mathbf{r})$ can be calculated from the negative gradient of the potential ϕ .

$$\mathbf{E}_{DC}(\mathbf{r}) = -\nabla\phi(\mathbf{r}) \tag{15}$$

If the point source current strength is I , is located at $\mathbf{r}_s = (x_s, y_s, z_s)$, and is obtained according to the continuity of the electric field by using the differential form of Ohm's law $\mathbf{j} = \sigma\mathbf{E}$, then

$$\nabla \cdot \mathbf{J}(\mathbf{r}) = I\delta(\mathbf{r} - \mathbf{r}_s) \tag{16}$$

where δ is the impulse function. The three-dimensional Poisson equation satisfied by the point source field can be obtained by



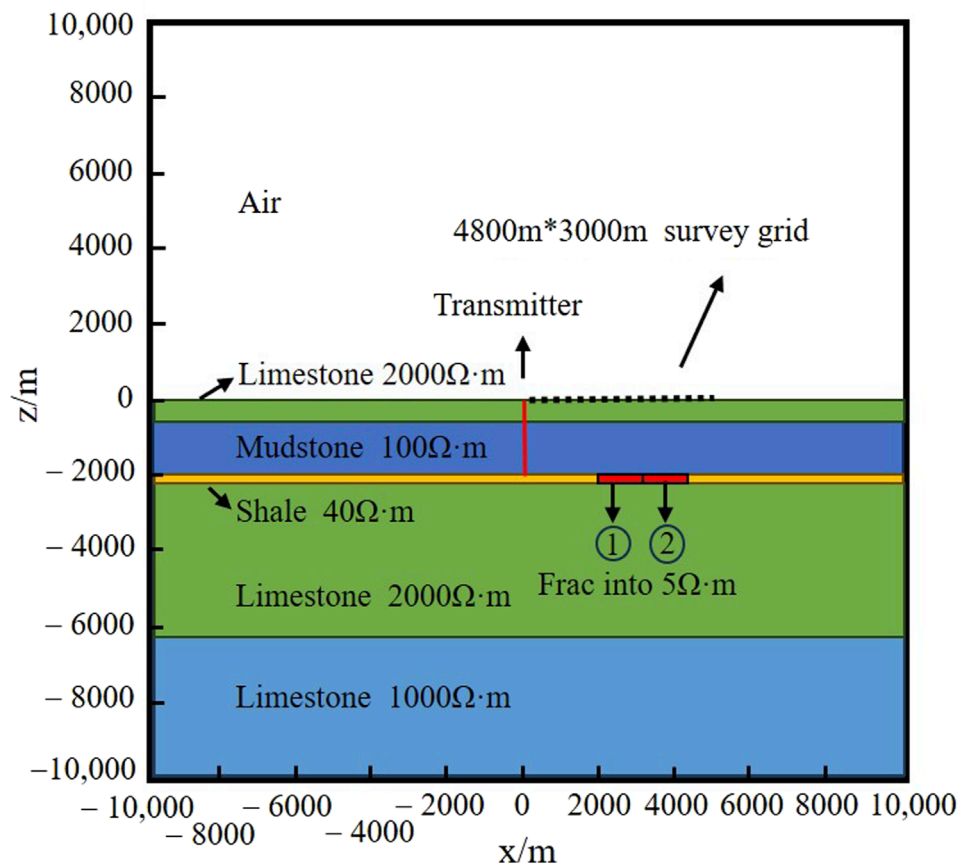


FIGURE 7 Schematic diagram of the shale fracturing model.

combining the above equations:

$$\nabla \cdot (\sigma \nabla \phi(\mathbf{r})) = -I\delta(\mathbf{r} - \mathbf{r}_s) \tag{17}$$

The same grid is used to ensure the consistency of the boundary between the direct current electric field and the vector electric field, and the total field method is used to solve both the direct current (DC) field and the transient electromagnetic field. Due to the large solution area, the Dirichlet boundary condition is applied to the external boundary Γ in the calculation process.

$$\phi|_{\Gamma} = 0, (\mathbf{n} \times \mathbf{E})|_{\Gamma} = 0 \tag{18}$$

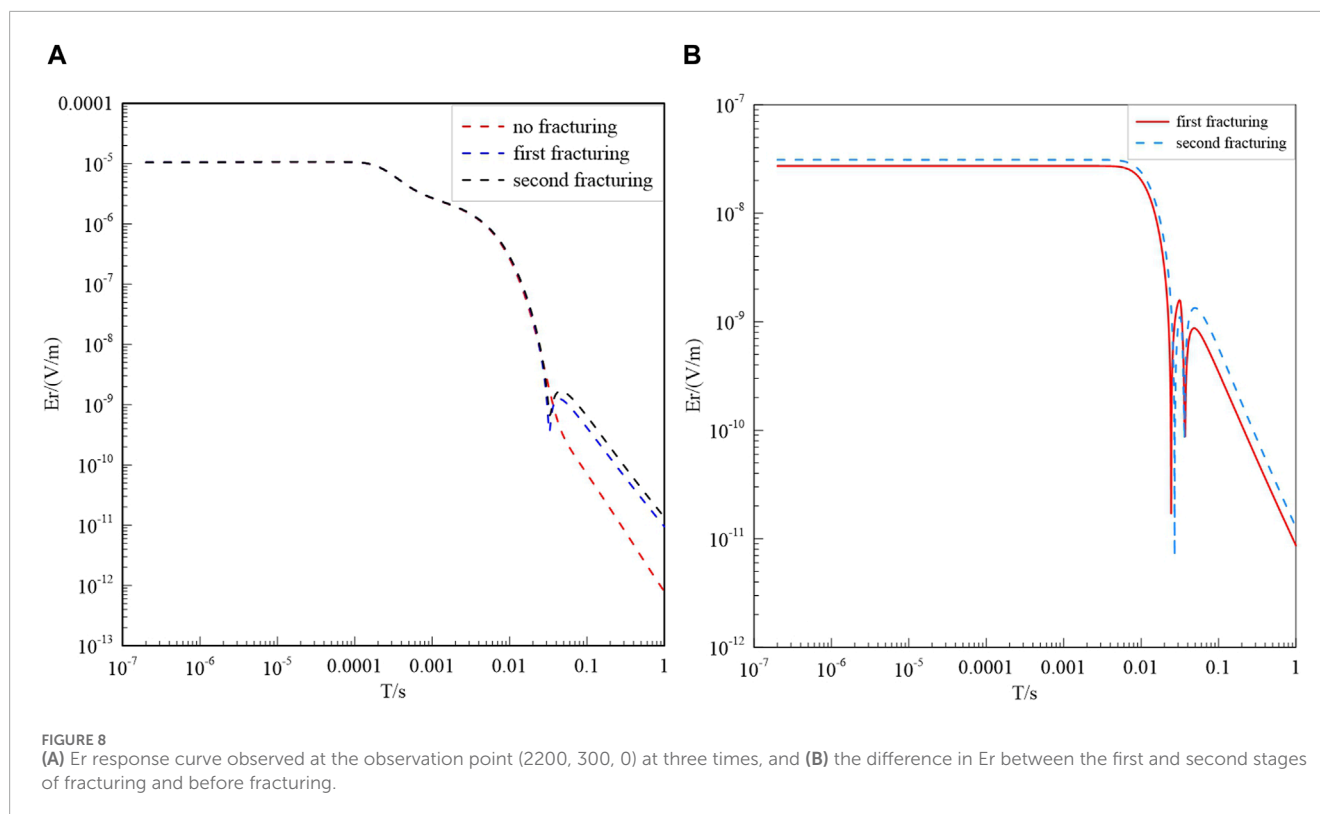
The tangential electric fields of the edges of all of the tetrahedrons are obtained using the lower-upper (LU) decomposition and quick back substitution of the above equations using a multi-wavefront direct solver; namely, the multifrontal massively parallel sparse direct solver (MUMPS). The electric field response E_x , E_y , and E_z at any point in space is obtained via linear interpolation of the basis function. The response of the magnetic field component is obtained using Faraday's law of electromagnetic induction.

4 Validation of three-dimensional model of time-domain electromagnetic method in borehole and on the ground

4.1 Verification of algorithm's accuracy

To validate the accuracy of the algorithm proposed in this paper, a comparison verification is conducted using a homogeneous half-space model. Assuming that the resistivity of air is $10^6 \Omega \cdot m$ and the resistivity of the homogeneous half-space is $100 \Omega \cdot m$, a vertical electric dipole with a depth range of 100 m–101 m underground is considered. The transmitting current is set to 1 A. The receiving point is located on the ground along the x-direction at a distance of 1,500 m from the transmitter. Schematic diagrams of the model and mesh partition are presented in Figure 3

The computational results of the homogeneous half-space are compared and analyzed against the results obtained using COMSOL (Zheng and Zhao, 2023). As shown in Figure 4, the finite element solution closely matches the curve obtained using COMSOL. Based on calculations, the relative error between the two is within $\pm 5\%$.



Therefore, it can be concluded that the algorithm proposed in this paper is reliable and trustworthy.

4.2 3-D model verification

To verify the computational accuracy of the algorithm for complex geoelectric models, a three-dimensional model (Liu Y. J. et al., 2020) is designed. The electrical source has a length of 1,000 m, is arranged along the y -direction, and its center point is located at the surface (0,0,0). The transmitting current is set to 1 A. Three measurement points are arranged along the x -direction, and they have coordinates of A (-500,0,0), B (-1050,0,0), and C (-2000,0,0). Local refinement is applied to the mesh at the transmitter and measurement points (Figure 5).

Figure 6 compares the numerical results of the electric field component E_y at the three measurement points with the finite volume calculation results of Liu et al. (Liu Y. J. et al., 2020). It can be observed from Figure 6 that the results fit well, with errors all less than 5%. This demonstrates the accuracy of the algorithm proposed in this paper.

5 Response analysis of shale gas fracturing monitoring model

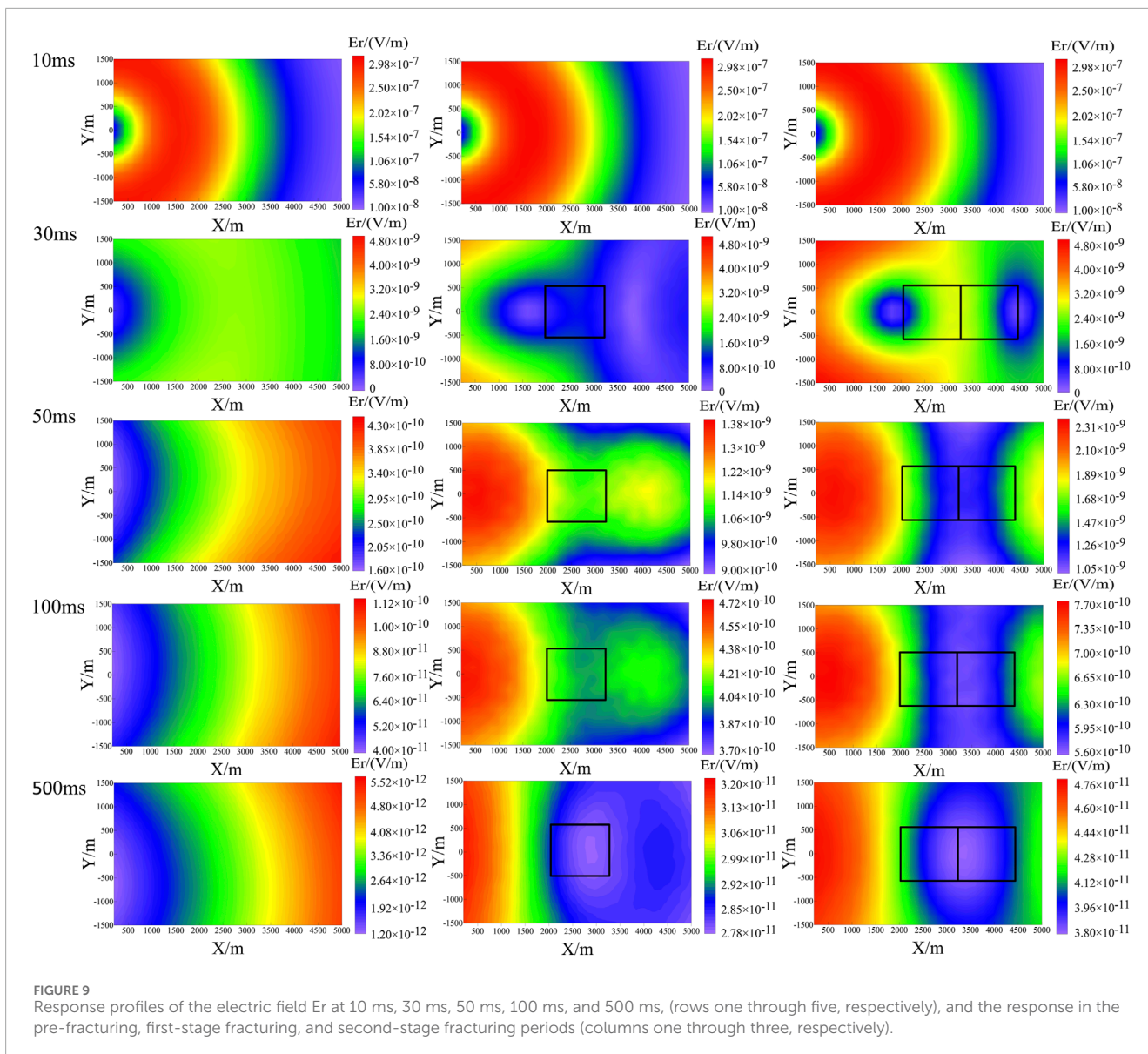
To theoretically explore the capability of the borehole transient electromagnetic method for the dynamic monitoring of shale gas hydraulic fracturing, a three-dimensional model (Figure 7) is designed. In this model, a layer of shale with a thickness of 300 m

and resistivity of 40 Ω -m is located 2000 m below sea level. Above the shale layer, there is limestone with a thickness of 700 m and a resistivity of 2000 Ω -m, as well as mudstone with a thickness of 1,300 m and resistivity of 100 Ω -m. Below the shale layer, a layer of limestone with a resistivity of 2000 Ω -m and thickness of 4,300 m overlies a limestone substrate with a resistivity of 1,000 Ω -m. The wellhead is located at (0,0), where a transmitting source with a length of 2000 m along the z -direction is deployed. The transmitting current is set to 1 A. The measurement points are distributed within an x range of 200 m–5,000 m and a y range of -1,500 m–1,500 m, with a mesh size of 200 m \times 200 m. Two hydraulic fracturing stages are conducted within the shale layer, each with a fracture range of 1,200 m \times 1,000 m \times 300 m. After fracturing, the resistivity changes to 5 Ω -m. Three observations are made at the surface to observe the response of the electric field before hydraulic fracturing, after the first fracturing stage, and after the second fracturing stage. The radial electric field E_r is analyzed.

$$E_r = \sqrt{E_x^2 + E_y^2} \quad (19)$$

Figure 8 shows the E_r response curve at observation point (2,200, 300, 0) and the difference curve between E_r after two hydraulic fracturing stages and before fracturing. It can be observed that significant changes in the electric field response E_r occur at 30 ms and 50 ms. To better illustrate the distribution pattern of the underground electric field at different times, the response profiles of the electric field E_r at 10 ms, 30 ms, 50 ms, 100 ms, and 500 ms are plotted in Figure 9.

Figure 9 displays the response profiles of the electric field E_r before and after fracturing at 10 ms, 30 ms, 50 ms,



100 ms, and 500 ms. It can be seen from Figure 9 that before fracturing, the contours of the electric field E_r are relatively smooth from the early to late stages, and the electric field response exhibits faster attenuation in the near field and slower attenuation in the far field. The contours of the electric field before and after fracturing are similar at 10 ms. After 10 ms, significant differences in the electric field response values can be observed between the first and second fracturing stages. After 30 ms, clear boundaries of the resistivity changes can be seen (Figure 9). At 500 ms, it is evident that the electric field values are smaller in the low-resistivity body than in the surrounding area, demonstrating the capability of this method in detecting anomalies.

To further analyze the changes in the electric field response values before and after hydraulic fracturing and to verify the applicability of this method in the dynamic monitoring of shale gas fracturing, we created difference profile maps of the electric

field response E_r at 10 ms, 30 ms, 50 ms, 100 ms, and 500 ms (Figure 10). As can be seen from Figures 10, at 10 ms, there is a significant change in the field values in the anomaly area, and the change is greater in the second fracturing stage compared to the first fracturing stage and is greater in the fracturing stages compared to no fracturing. The size and location of the anomaly body can be distinguished based on the field values. At 30 ms, the decay rate of the electric field values E_r near the anomaly body is slower than that without fracturing. Similarly, it can be observed that the decay rate of the electric field response values E_r near the anomaly is slower in the second fracturing stage than in the first fracturing stage. This is because the shale becomes a low-resistivity body after fracturing, leading to a decrease in its resistivity and the formation of significant current pathways in the low-resistivity body, resulting in significant changes in the electric field in the fracturing area. In the late stage, the residual values near the low-resistivity body are smaller than those in the

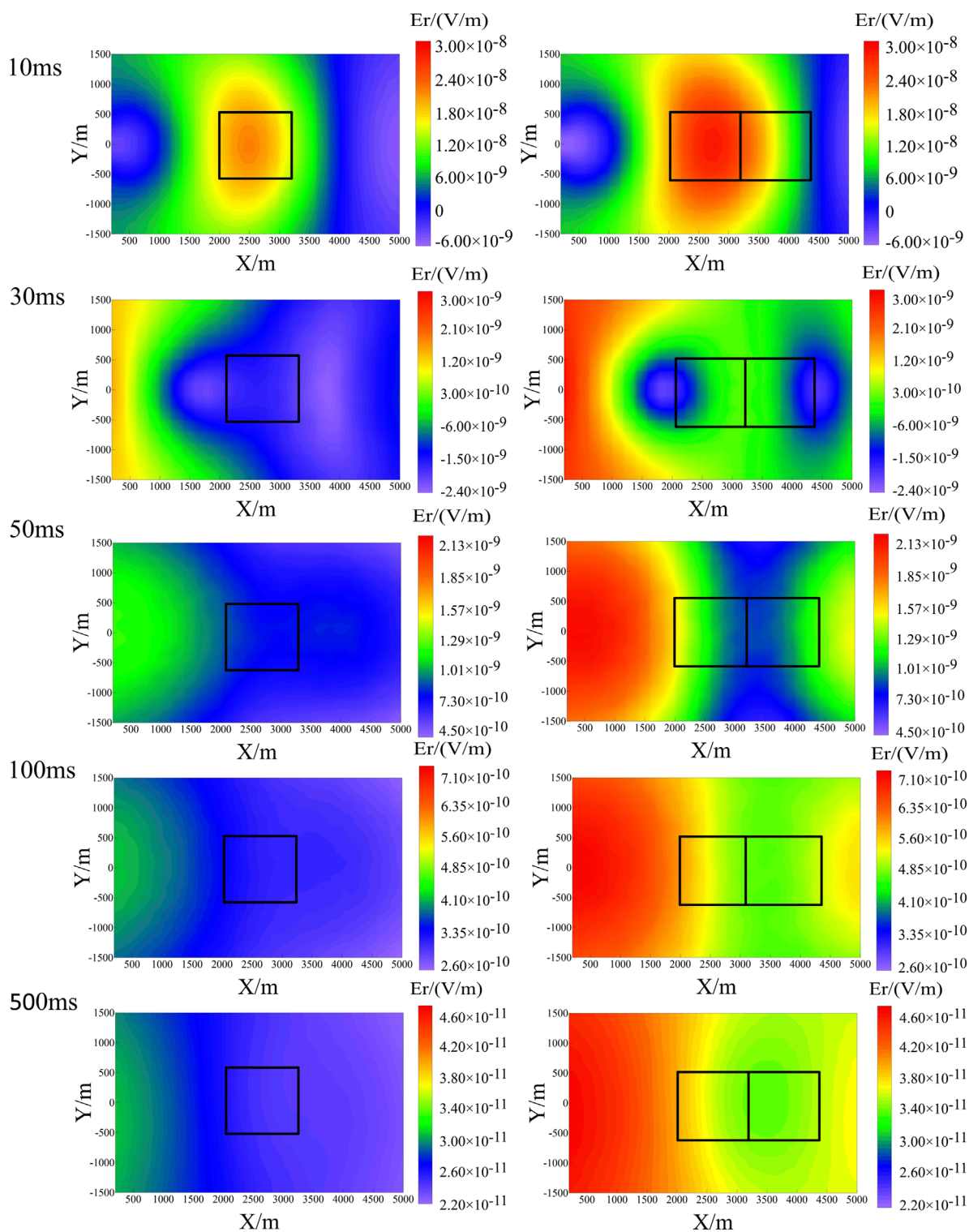


FIGURE 10 Response profiles of the electric field E_r fracturing differential value in the first stage (column one) and second stage (column two) of E_r fracturing at 10 ms, 30 ms, 50 ms, 100 ms, and 500 ms (rows one through five, respectively).

surrounding area, which is consistent with the decay law of the electromagnetic field near the low-resistivity body. In conclusion, based on the contour maps of E_r and the residual contour maps of E_r ,

the significant changes in the electric field response before and after hydraulic fracturing in a shale gas reservoir can be clearly observed, confirming the effectiveness and feasibility of using the borehole

transient electromagnetic method for dynamic monitoring of shale gas fracturing.

6 Conclusion

In this study, we applied the unstructured vector finite element method to three-dimensional forward simulation of the borehole transient electromagnetic (TEM) method for the dynamic monitoring of shale gas fracturing. The effectiveness of the borehole TEM method in monitoring the dynamic changes in underground mineral deposits and oil and gas reservoirs with resistivity differences was demonstrated. Based on the analysis of the response, the following conclusions were attained:

- (1) Under the condition of a homogeneous half-space, the algorithm's correctness was verified by comparing the finite element solution proposed in this study with the COMSOL solution. To further validate the accuracy of the algorithm, comparisons were made with the finite volume method in surface mode. It was demonstrated that the algorithm can effectively perform three-dimensional forward simulations of the borehole TEM method in complex models.
- (2) Numerical analysis of underground shale gas reservoir models revealed that the borehole TEM method can effectively characterize the electrical differences before and after shale gas fracturing, thereby achieving high-precision dynamic monitoring of shale gas fracturing.

At present, many scholars have carried out the research of borehole to ground transient electromagnetic method, but it is rarely applied to the dynamic monitoring of shale gas fracturing. With the help of this algorithm proposed in this study allows for the analysis of the patterns of the borehole TEM method in the dynamic monitoring of unconventional oil and gas fracturing. This provides theoretical guidance for the dynamic monitoring of unconventional oil and gas fracturing in practical production processes.

Data availability statement

The original contributions presented in the study are included in the article/Supplementary Material, further inquiries can be directed to the corresponding author.

References

- Ansari, S., and Farquharson, C. G. (2014). 3D finite-element forward modeling of electromagnetic data using vector and scalar potentials and unstructured grids. *Geophysics* 79, 149–165. doi:10.1190/geo2013-0172.1
- Commer, M., Helwig, S. L., Hördt, A., Scholl, C., and Tezkan, B. (2006). New results on the resistivity structure of Merapi Volcano (Indonesia), derived from three-dimensional restricted in version of long-offset transient electromagnetic data. *Geophys. J. Int.* 167, 1172–1187. doi:10.1111/j.1365-246x.2006.03182.x
- Cuevas, N. (2012). "Casing effect in borehole-surface (surface-borehole) EM fields," in 74th Annual International Conference and Exhibition, EAGE//Extended Abstracts, P201.
- Ghada, M. S., and Al-Najim, F. A. (2015). The transient electromagnetic field created by electric line source on a plane conducting Earth. *Int. J. Mech. Appl.* 5, 16–22. doi:10.5923/j.mechanics.20150501.03
- Haroony, A., Adrian, J., Bergers, R., Gurk, M., Tezkan, B., Mammadov, A. L., et al. (2015). Joint inversion of long-offset and central-loop transient electromagnetic data: application to a mud volcano exploration in Perekishkul, Azerbaijan. *Geophys. Prospect.* 63, 478–494. doi:10.1111/1365-2478.12157
- He, J. S., and Xue, G. Q. (2018). Review of the key techniques on short-offset electromagnetic detection. *Chin. J. Geophys.* 61, 1–8. doi:10.6038/cig2018L0003
- Hördt, A., Druskin, V. L., Knizhnerman, L. A., and Strack, K. M. (1992). Interpretation of 3-D effects in long-offset transient electromagnetic (LOTTEM) soundings in the Münsterland area/Germany. *Geophysics* 57, 1127–1137. doi:10.1190/1.1443327
- Hu, W. B., Shen, J. S., and Yan, L. J. (2022). *Principle and application of controllable source electromagnetic method for reservoir fluid prediction*. China: Science Press.

Author contributions

WZ: Conceptualization, Formal Analysis, Methodology, Software, Writing–original draft. XX: Conceptualization, Methodology, Resources, Writing–review and editing. LZ: Formal Analysis, Resources, Writing–review and editing. XW: Software, Validation, Writing–review and editing. LY: Supervision, Writing–review and editing.

Funding

The author(s) declare that financial support was received for the research, authorship, and/or publication of this article. This research was funded by the National Natural Science Foundation of Key Project of China, grant number 42030805; the National Natural Science Foundation of China, grant number 42274103; and the Science and Technology Department Project of China Petroleum & Chemical Corporation, grant number P22163.

Conflict of interest

The authors declare that the research was conducted in the absence of any commercial or financial relationships that could be construed as a potential conflict of interest.

The authors declare that they have no known competing financial interests or personal relationships that could have appeared to influence the work reported in this paper.

Publisher's note

All claims expressed in this article are solely those of the authors and do not necessarily represent those of their affiliated organizations, or those of the publisher, the editors and the reviewers. Any product that may be evaluated in this article, or claim that may be made by its manufacturer, is not guaranteed or endorsed by the publisher.

- Hu, Z. Z., He, Z. X., Li, D. C., Liu, Y. X., Sun, W. B., Wang, C. F., et al. (2014). Reservoir monitoring feasibility study with time lapse magnetotellurics survey in Sebei Gas Field. *Oil Geophys. Prospect.* 49, 997–1005. doi:10.13810/j.cnki.issn.1000-7210.2014.05.051
- Ke, G. P., and Huang, Q. H. (2009). 3D forward and inversion problems of borehole-to-surface electrical method. *Acta Sci. Nat. Univ. Pekin.* 45, 264–272. doi:10.13209/j.0479-8023.2009.041
- Keller, G. V., Pritchard, J. I., Jacobson, J. J., and Harthill, N. (1984). Megasource time-domain electromagnetic sounding methods. *Geophysics* 49, 993–1009. doi:10.1190/1.1441743
- Li, J. H., He, Z. X., and Xu, Y. X. (2017). Three-dimensional numerical modeling of surface-to-borehole electromagnetic method for monitoring reservoir. *Appl. Geophysics* 14, 101–111. doi:10.1007/s11770-017-0643-8
- Liu, R., Liu, J., Wang, J., Liu, Z., and Guo, R. W. (2020a). A time-lapse CSEM monitoring study for hydraulic fracturing in shale gas reservoir. *Mar. Petroleum Geol.* 120, 104545. doi:10.1016/j.marpetgeo.2020.104545
- Liu, Y. J., Yogeshwar, P., Hu, X. Y., Peng, R. H., Tezkan, B., Mörbe, W., et al. (2020b). Effects of electrical anisotropy on long-offset transient electromagnetic data. *Geophys. J. Int.* 222, 1074–1089. doi:10.1093/gji/ggaa213
- Mitsuhashi, Y. J., Uchida, T., and Amano, H. (2002). 2.5-D in-version of frequency-domain electromagnetic data generated by a grounded-wire source. *Geophysics* 67, 1753–1768. doi:10.1190/1.1527076
- Müller, M., Hördt, A., and Neubauer, F. (2002). Internal structure of Mount Merapi, Indonesia, derived from long-offset transient electromagnetic data. *J. Geophys. Res. Solid Earth* 107. doi:10.1029/2001jb000148
- Orange, A., Key, K., and Constable, S. (2009). The feasibility of reservoir monitoring using time-lapse marine CSEM. *Geophysics* 74, 21–29. doi:10.1190/1.3059600
- Peng, R. H., Hu, X. Y., Liu, Y. X., and He, Z. X. (2012). “The feasibility study of time-lapse two dimensional magnetotelluric for reservoir monitoring,” in The 28th Annual Meeting of the Chinese Geophysical Society, Beijing, China.
- Strack, K. M. (1984). The deep transient electromagnetic sounding technique: first field test in Australia. *Explor. Geophys.* 15, 251–259. doi:10.1071/eg984251
- Um, E. S., Harris, J. M., and Alumbaugh, D. L. (2010). 3D time-domain simulation of electromagnetic diffusion phenomena: a finite-element electric-field approach. *Geophysics* 75, 115–126. doi:10.1190/1.3473694
- Wang, X. Y., Yan, L. J., and Mao, Y. R. (2022). Simulation and analysis of dynamic monitoring of oil and gas reservoir based on grounded electric source TEM. *Oil Geophys. Prospect.* 57, 459–466. doi:10.13810/j.cnki.issn.1000-7210.2022.02.023
- Wang, Z. G., He, Z. X., and Liu, Y. (2006). Research of three-dimension modeling and anomalous rule on borehole-ground DC method. *Chin. J. Eng. Geophys.* 3, 87–92.
- Wang, Z. G., He, Z. X., and Wei, W. B. (2007). Research on 3D modeling of borehole vertical bipole using body integral equation. *Prog. Geophys.* 22, 1802–1808.
- Wirianto, M., Mulder, W. A., and Slob, E. C. (2010). A feasibility study of land CSEM reservoir monitoring in a complex 3-D model. *Geophys. J. International* 181, 741–755. doi:10.1111/j.1365-246x.2010.04544.x
- Xie, X. B., Zhou, L., Yan, L. J., and Hu, W. B. (2016). Remaining oil detection with time-lapse long offset& window transient electromagnetic sounding. *Oil Geophys. Prospect.* 51, 605–612. doi:10.13810/j.cnki.issn.1000-7210.2016.03024
- Zhang, J. Q. (2018). *Finite-length wire Source 3D electromagnetic forward modeling of vertical*. Beijing, China: China University of Geosciences.
- Zhao, P. Q., Hao, H. M., Ni, T. L., Li, H. G., Tao, Z. Q., and Ma, Y. H. (2019). A novel technology: reservoir seepage geophysics. *Oil Geophys. Prospect.* 54, 719–728. doi:10.13810/j.cnki.issn.1000-7210.2019.03.028
- Zheng, H. B., and Zhao, X. M. (2023). Application of transient electromagnetic method based on COMSOL simulation in tunnel advance geological prediction. *Highway* 68, 469–474.